atoms

MDPI

*Communication*

# Lithium-like $O^{5+}$ Emission near 19 Å

**Jaan K. Lepson [1,*], Gregory V. Brown [2], Joel H. T. Clementson [2], Alexander J. Fairchild [2], Ming Feng Gu [1], Natalie Hell [2], Elmar Träbert [2,3] and Peter Beiersdorfer [1,2]**

1 Space Sciences Laboratory, University of California, Berkeley, CA 94720, USA; beiersdorfer@berkeley.edu (P.B.)
2 Physics Division, Lawrence Livermore National Laboratory, Livermore CA 94550, USA; brown86@llnl.gov (G.V.B.)
3 Fakultät für Physik und Astronomie, Ruhr-Universität Bochum, 44780 Bochum, Germany
* Correspondence: lepson@berkeley.edu

**Abstract:** Using a high-resolution grating spectrometer on the Livermore EBIT-I electron beam ion trap, we have measured three $n = 3, 4 \rightarrow n = 1$ K-shell emission lines in lithium-like $O^{5+}$, which are situated near the O VIII Lyman-$\alpha$ lines at 19 Å. Two of the resulting wavelengths agree well with the wavelengths of these lines we reported earlier, but the wavelength of the third line does not. In contrast, our new wavelengths now fully agree with those from resonant photo-absorption experiments on the PETRA III synchrotron facility.

**Keywords:** X-ray spectra; highly charged ions; electron beam ion trap; K-shell emission; oxygen

check for updates

Academic Editors: John Sheil and Ronnie Hoekstra

Received: 28 October 2024
Revised: 27 December 2024
Accepted: 17 January 2025
Published: 21 January 2025

**Citation:** Lepson, J.K.; Brown, G.V.; Clementson, J.H.T.; Fairchild, A.J.; Gu, M.F.; Hell, N.; Träbert, E.; Beiersdorfer, P. Lithium-like $O^{5+}$ Emission near 19 Å. *Atoms* **2025**, *13*, 10. https://doi.org/10.3390/atoms13020010

**Correction Statement:** This article has been republished with a minor change. The change does not affect the scientific content of the article and further details are available within the backmatter of the website version of this article.

**Copyright:** © 2025 by the authors. Licensee MDPI, Basel, Switzerland. This article is an open access article distributed under the terms and conditions of the Creative Commons Attribution (CC BY) license (https://creativecommons.org/licenses/by/4.0/).

## 1. Introduction

Notably, the strongest collisionally excited $n = 3 \rightarrow n = 1$ lines of lithium-like N V and O VI appear on the long-wavelength side of the respective N VII and O VIII Lyman-$\alpha$ lines [1,2]. By contrast, in higher-Z ions (for example, in argon, chromium, and iron [3–5]), they appear on the long-wavelength side of the helium-like K$\beta$ lines. Moreover, in the case of nitrogen, the sum of the two strongest $n = 3 \rightarrow n = 1$ lines is about 1/5 of the strength of the two strongest $n = 2 \rightarrow n = 1$ collisionally excited lithium-like lines [2], i.e., the $1s2s2p\ ^2P_{1/2,3/2} \rightarrow 1s^2 2s\ ^2S_{1/2}$ transitions, commonly labeled $r$ and $q$. Because the $n = 3 \rightarrow n = 1$ lines of lithium-like N V and O VI can provide valuable information on the charge balance and are less blended than the corresponding $n = 2 \rightarrow n = 1$ lines, they are important for spectral analysis, especially of astrophysical plasmas, enabling us to identify these lines and have accurate position information.

The wavelengths of the two strongest $n = 3 \rightarrow n = 1$ lines of O VI, which fall into the wavelength region between 19.1 and 19.4 Å, were recently measured using resonant photo-absorption at the PETRA III synchrotron facility and the Heidelberg portable electron beam ion trap [6], as well as by subsequently using emission line spectroscopy with a high-resolution grating spectrometer on the Livermore EBIT-I electron beam ion trap [1]. Excellent agreement between the two types of measurements was found for two of the lines. However, the measured wavelengths of the third line disagreed within four standard deviations, i.e., by 3.7 +/− 0.9 mÅ.

To understand what may have caused this discrepancy, we have repeated our emission line measurements with an improved focus of our spectrometer. We have also reconsidered our calibration procedures. In the following, we present our new measurements and the updated wavelength results.

## 2. Measurement

Measurements were performed on the EBIT-I ("ebit-one") electron beam ion trap, which has been in continuous use for spectroscopic measurements since 1986 [7–9]. In this experiment, we used an experimental procedure employed before [1,10,11].

Oxygen was introduced into the trap via a ballistic gas injector in the form of carbon dioxide. Continuous injection of neutral $CO_2$ ensures that lower charge states of oxygen are abundantly present even if the high beam energy ($\leq$8 keV) would otherwise produce bare oxygen. The magnetically compressed electron beam dissociates the molecule and ionizes the oxygen atom. It then excites the ions and thus produces line emission primarily by electron-impact excitation. The oxygen K-shell emission was dispersed by a high-resolution grazing incidence spectrometer [12,13], and the X-rays were recorded with a liquid nitrogen cooled charge-coupled device (CCD) with 1340 $\times$ 1300 pixels of 20 µm $\times$ 20 µm nominal size. We note that charge exchange can also produce line emission. However, charge exchange happens as neutral gas interacts with the extended ion cloud and, therefore, the resulting emission would show up in the grating spectrometer spectrum as a broad halo surrounding the sharply localized emission from electron-impact excitation. Such a halo, however, is not seen.

We made measurements about two years apart with different settings of the spectrometer: (1) 15 Å to about 22 Å and (2) 16 Å to about 23 Å. A typical spectrum of the oxygen emission lines in the 16 to 23 Å region is shown in Figure 1. In both cases, these settings allowed us to see the $3p \rightarrow 1s$ Ly-$\beta$ line of hydrogen-like O VIII at 16 Å at the short-wavelength side, and the $1s2s\ ^3S_1 \rightarrow 1s^2\ ^1S_0$ "forbidden" line of helium-like O VII, commonly denoted as $z$, at 22 Å at the long-wavelength side.

The lines from helium- and hydrogen-like oxygen served as our calibration references. Other reference lines we employed were the $1s2p\ ^1P_1 \rightarrow 1s^2\ ^1S_0$ "resonance" line and the $1s2p\ ^3P_1 \rightarrow 1s^2\ ^1S_0$ "intercombination" line of helium-like O VII (denoted as $w$ and $y$, respectively) and the $1snp\ ^1P_1 \rightarrow 1s^2\ ^1S_0$ $(n = 3 - 6)$ lines of helium-like O VII (denoted here as the K$\beta$, K$\gamma$, K$\delta$, and K$\epsilon$ lines, respectively). We also employed the $2p \rightarrow 1s$ Ly-$\alpha$ line and the $2p \rightarrow 1s$ Ly-$\gamma$ line, when available, of hydrogen-like O VIII as a calibration reference.

The spectrum in Figure 1 also shows the two $n = 3 \rightarrow n = 1$ O VI lines of interest. The lines are well resolved and can be seen near 19.2 and near 19.4 Å. They are labeled as $A$ and $B$ in Figure 1. A third O VI line of interest, which we label C, is formed by $n = 4 \rightarrow n = 1$ transitions and is situated on the short-wavelength shoulder of the O VII K$\beta$ line. It is too weak to unequivocally discern in Figure 1. In total, we were able to fit Lines A and B in 14 spectra, and Line C in a total of 12 measurement files. Each of these spectra was recorded for 60 min.

The wavelengths of the O VII and O VIII lines are known from theory [14–19] to better than 1 mÅ [20,21]. Thus, they serve as high-quality in situ calibration references.

Unfortunately, the O VIII lines are a blend of the two fine structure components comprising each line. Consequently, we have to make assumptions as to the relative amplitude of each component. The relative ratio of the two $np_{1/2,3/2} \rightarrow 1s_{1/2}$ fine structure components by the statistical weights of the levels is 1:2. However, a line excited by the mono-directional electron beam may be polarized. In fact, the linear polarization of the $np_{3/2} \rightarrow 1s_{1/2}$ component may approach +50 % at certain energies (even higher at the excitation threshold) [22]. By contrast, the $np_{1/2} \rightarrow 1s_{1/2}$ component is unpolarized at any beam energy. Using these extremes, the ratio of the fine structure components may, therefore, shift from 1:2 to 1:2.4. This effect shifts the value of the wavelength assigned to these reference lines. In the case of the Lyman-$\alpha$ line, where the effect is the strongest, the shift is from 18.96891 Å to 18.96870 Å, or $-0.21$ mÅ. Luckily, this shift is relatively small, but it needs to be accounted for and limits the accuracy of the measurements if it is not. If the polarization was reduced from 50% to 40%, this correction would be $-0.17$ mÅ.

We take the uncertainty in the polarization correction to be the difference between the two values, i.e., −0.044 mÅ, which contributes an almost negligible uncertainty to our measurements. The correction affecting the Lyman-$\beta$ line is much smaller, i.e., −0.04 mÅ, and is thus almost negligible as well.

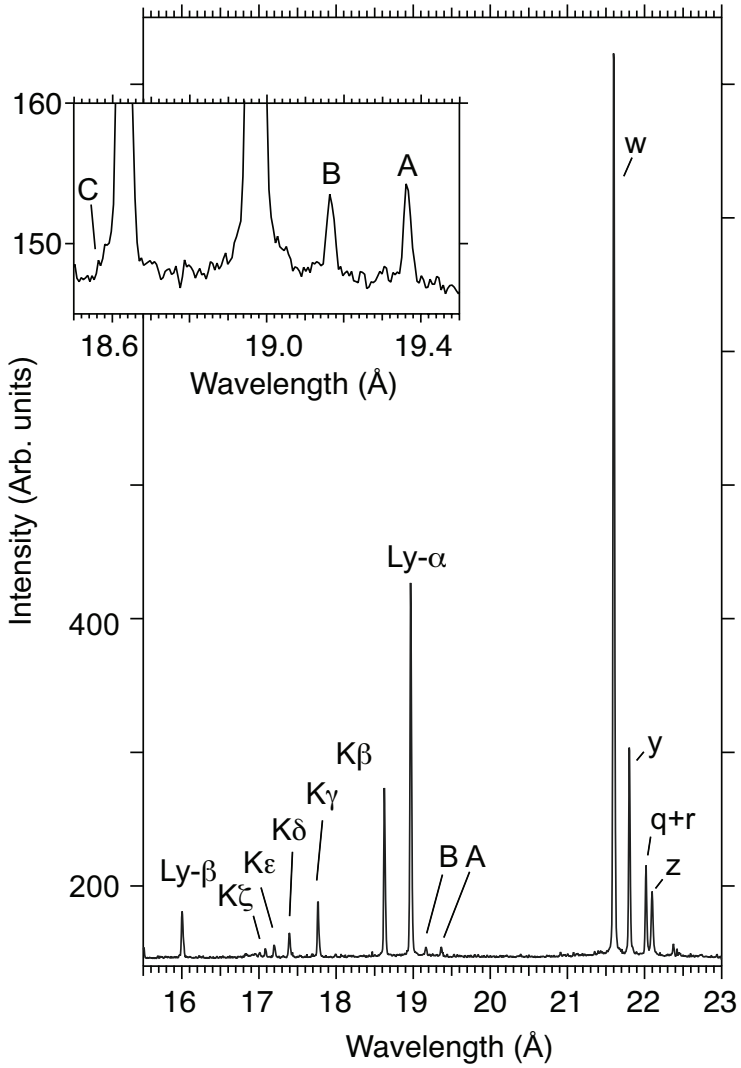



**Figure 1.** Spectrum of the K-shell emission lines of oxygen measured on the EBIT-I electron beam ion trap at Livermore. Besides the O VIII Lyman-$\alpha$ and Lyman-$\beta$ transition, the spectrum shows the $1snp\ ^1P_1 \rightarrow 1s^2\ ^1S_0$ Rydberg series lines of O VII, labeled K$\beta$ through K$\zeta$. The $n = 2 \rightarrow n = 1$ O VII transitions are labeled $w$, $y$, and $z$, and the $n = 2 \rightarrow n = 1$ O VI transitions are labeled $q$ and $r$. The two strongest $n = 3 \rightarrow n = 1$ O VI features of interest are labeled A ($1s2s3p \rightarrow 1s^22s$) and B ($1s2s3p \rightarrow 1s^22s$); Line C is labeled on the inset.

Because new calculations [19] became available since our original measurement of oxygen data in 2022, we reworked the list of reference wavelengths. When doing so, we discovered that we made a typo in the reference wavelength used for the O VIII Lyman-$\alpha$ line in the 2022 paper [1]. Instead of 18.9687 Å, we inadvertently used 18.9696 Å for the reference value of the Lyman-$\alpha$ line, i.e., a value that was 0.9 mÅ (!) larger than it should have been. Correcting for this typographical error reduces the previously measured wavelength of Line B by 0.8 mÅ. The measured O VI wavelengths from the 2022 paper [1] after they were corrected for this error are given in Table 1.

**Table 1.** Comparisons of measured and predicted K-shell lines of O VI. All transitions are to the $1s^2 2s_{1/2}$ lower level; only the two dominant components are shown. All wavelenths are in units of Å.

| Key | Upper Level (J) | $\lambda_{exp}$ TKS(2020) [a] | $\lambda_{exp}$ BG(2022) [b] | $\lambda_{exp}$ Present Work [c] | $\lambda_{theo}$ MBPT [d] |
|---|---|---|---|---|---|
| A | $1s_{1/2}2s_{1/2}3p_{3/2}(\frac{1}{2})$, $1s_{1/2}2s_{1/2}3p_{3/2}(\frac{3}{2})$ | 19.3665(6) | 19.3658(7) | 19.3653(6) | 19.3666 |
| B | $1s_{1/2}2s_{1/2}3p_{1/2}(\frac{1}{2})$, $1s_{1/2}2s_{1/2}3p_{3/2}(\frac{3}{2})$ | 19.1641(6) | 19.1670(6) | 19.1650(6) | 19.1656 |
| C | $1s_{1/2}2s_{1/2}4p_{3/2}(\frac{3}{2})$, $1s_{1/2}2s_{1/2}4p_{3/2}(\frac{1}{2})$ | 18.5833(8) | 18.5852(19) | 18.5833(39) | 18.5841 |

[a] Togawa, Kühn, Shah et al. [6]; numbers in parentheses are uncertainties in tenths of mÅ. [b] Beiersdorfer and Gu [1] (corrected as discussed in the text); numbers in parentheses are uncertainties in tenths of mÅ. [c] Numbers in parentheses are uncertainties in tenths of mÅ. [d] Intensity-weighted average wavelength calculated with the many-body perturbation theory option of the Flexible Atomic Code. See text.

Table 1 also lists the wavelengths of the three observed O VI features that we newly determined from our measurements, as well as the results from the older synchrotron measurements by Togawa et al. [6]. A graphical summary of values listed in Table 1 is also given in Figure 2. In this figure, we also show the weighted average of the three measurements for each line, which is indicated its the upper and lower uncertainty limits.

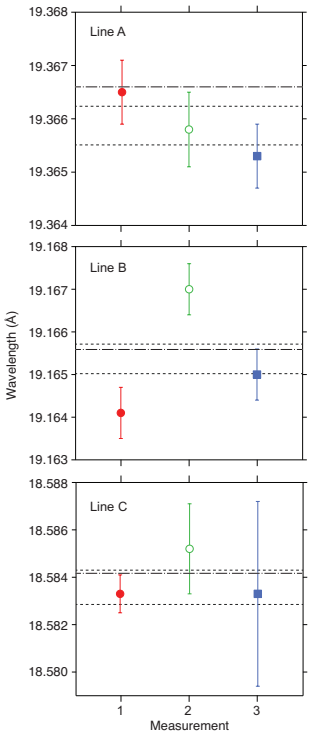



**Figure 2.** Comparisons of measured and predicted K-shell lines of O VI. Here, the measurements by Togawa et al. [6] are shown in red (solid circles), and those by Beiersdorfer et al. [1] are shown in green (open circles). The present measurements are shown in blue (solid squares). The uncertainty-weighted average of the measurements of each line is indicated by the band enclosed by its upper and lower uncertainties, which are shown as dashed lines. The theoretical value is given by the dot-dashed line.

## 3. Results and Discussion

As seen from the data in Table 1 and Figure 2, our new measurements agree well with those from Togawa et al. [6]. In particular, the original discrepancy of nearly 4 mÅ (or 3 mÅ after correcting for the inadvertent error in the reference wavelength) that existed between the 2022 measurement of Line B and the result from Togawa et al. [6] was reduced

to 1 mÅ, which is within the uncertainties of the respective measurements.In fact, when compared to the weighted average of all three measurements of Line B, the measurement of Beiersdorfer et al. [1] is about as close to the weighted average as the measurement of Togawa et al. [6], and both measurements are within about one standard deviation from the uncertainty band of the weighted average. This is, of course, a reflection of the fact that our new measurement lies approximately between those two earlier results. However, this shows that the earlier disagreement should be treated as a result of statistics rather than the result of unknown systematic errors.

Our measurements of Lines A and C are in excellent agreement with our older EBIT-I results. However, the uncertainty associated with our new measurement of Line C is much higher than before because of the diminished brightness of the O VI line relative to the O VII line with which it blends. In other words, the charge balance in our current measurements favored O VII and O VIII. Blending with these higher charge states is not an issue for Lines A and B, and thus their uncertainties are almost an order of magnitude lower than that of Line C.

Finally, Table 1 also lists the wavelengths predicted using the many-body perturbation theory (MBPT) option in the Flexible Atomic Code [23,24]. MBPT results are also shown in Figure 2. The full set of MBPT data for O VI K-shell transitions has been reported before [1]. The wavelength values we provide for the lines in Table 1 and Figure 2 are based on these data and take into account the fact that each line is comprised multiple O VI transitions; only the dominant two transitions are given in Table 1, which, however, comprise at least 80% of the total intensity of the measured feature. The intensity of each transition contributing to a given line was computed in [1] with a collisional-radiative model constructed with data from the Flexible Atomic Code. Comparing the intensity-weighted MBPT wavelengths with our new data and those from [6] shows that both measurements are equally close to the theoretical predictions, differing on average by about 0.8 mÅ, which is within the uncertainties of the measurements.

**Author Contributions:** Experiment, A.J.F., N.H., P.B. and G.V.B.; methodology, P.B.; computation, M.F.G.; data analysis and curation, J.K.L., P.B. and E.T.; resources, P.B.; writing—original draft preparation, J.K.L. and P.B.; writing—review and editing, J.K.L., J.H.T.C., E.T., M.F.G., A.J.F., N.H., P.B. and G.V.B.; funding acquisition, P.B. All authors have read and agreed to the published version of the manuscript.

**Funding:** This work was supported by NASA's Astrophysics Research and Analysis Program under grant No. 80NSSC20K0832. The measurements were performed under the auspices of the U. S. Department of Energy by Lawrence Livermore National Laboratory under contract No. DE-AC52-07NA27344.

**Data Availability Statement:** The original contributions presented in this study are included in the article. Further inquiries can be directed to the corresponding authors.

**Conflicts of Interest:** The authors declare no conflicts of interest.

## References

1. Beiersdorfer, P.; Gu, M.F. K-shell Emission from O VI Near 19 Å. *Astrophys. J.* **2022**, *931*, 49. [CrossRef]
2. Lepson, J.K.; Beiersdorfer, P.; Gu, M.F.; Hell, N.; Brown, G.V. K-shell X-Ray Emission from Lithium-like Nitrogen N V. *Astrophys. J.* **2024**, *962*, 130. [CrossRef]
3. Smith, A.J.; Bitter, M.; Hsuan, H.; Hill, K.W.; von Goeler, S.; Timberlake, J.; Beiersdorfer, P.; Osterheld, A. K$\beta$ spectra of heliumlike iron from tokomak-fusion-test-reactor plasmas. *Phys. Rev. A* **1993**, *47*, 3073. [CrossRef] [PubMed]
4. Beiersdorfer, P.; Osterheld, A.L.; Phillips, T.W.; Bitter, M.; Hill, K.W.; von Goeler, S. High-resolution measurement, line identification, and spectral modeling of the K$\beta$ spectrum of heliumlike $Ar^{16+}$. *Phys. Rev. E* **1995**, *52*, 1980. [CrossRef] [PubMed]

5. Decaux, V.; Beiersdorfer, P.; Osterheld, A.; Chen, M.; Kahn, S.M. High-Resolution Measurements of the K alpha Spectra of Low-Ionization Species of Iron: A New Spectral Signature of Nonequilibrium Ionization Conditions in Young Supernova Remnants. *Astrophys. J.* **1995**, *443*, 464. [CrossRef]
6. Togawa, M.; Kühn, S.; Shah, C.; Amaro, P.; Steinbrügge, R.; Stierhof, J.; Hell, N.; Rosner, M.; Fujii, K.; Bissinger, M.; et al. Observation of strong two-electron-one-photon transitions in few-electron ions. *Phys. Rev. A* **2020**, *102*, 052831. [CrossRef]
7. Beiersdorfer, P.; Behar, E.; Boyce, K.R.; Brown, G.V.; Chen, H.; Gendreau, K.C.; Graf, A.; Gu, M.F.; Harris, C.L.; Kahn, S.M.; et al. Overview of the Livermore electron beam ion trap project. *Nucl. Instrum. Meth. Phys. Res. B* **2003**, *205*, 173–177. [CrossRef]
8. Marrs, R.E. Milestones in EBIT spectroscopy and why it almost did not work. *Can. J. Phys.* **2008**, *86*, 11. [CrossRef]
9. Beiersdorfer, P. A "brief" history of spectroscopy on EBIT. *Can. J. Phys.* **2008**, *86*, 1. [CrossRef]
10. Schmidt, M.; Beiersdorfer, P.; Chen, H.; Thorn, D.; Träbert, E.; Behar, E. Laboratory Wavelengths of K-Shell Resonance Lines of O V and O VI. *Astrophys. J.* **2004**, *604*, 562. [CrossRef]
11. Gu, M.F.; Schmidt, M.; Beiersdorfer, P.; Chen, H.; Thorn, D.B.; Träbert, E.; Behar, E.; Kahn, S.M. Laboratory Measurement and Theoretical Modeling of K-Shell X-Ray Lines from Inner-Shell Excited and Ionized Ions of Oxygen. *Astrophys. J.* **2005**, *627*, 1066–1071. [CrossRef]
12. Beiersdorfer, P.; Magee, E.W.; Träbert, E.; Chen, H.; Lepson, J.K.; Gu, M.F.; Schmidt, M. Flat-field grating spectrometer for high-resolution soft x-ray and extreme ultraviolet measurements on an electron beam ion trap. *Rev. Sci. Instrum.* **2004**, *75*, 3723. [CrossRef]
13. Beiersdorfer, P.; Magee, E.W.; Brown, G.V.; Hell, N.; Träbert, E.; Widmann, K. Extended-range grazing-incidence spectrometer for high-resolution extreme ultraviolet measurements on an electron beam ion trap. *Rev. Sci. Instrum.* **2014**, *85*, 11E422. [CrossRef]
14. Garcia, J.D.; Mack, J.E. Energy Level and Line Tables for One-Electron Atomic Spectra. *J. Opt. Soc. Am.* **1965**, *55*, 654. [CrossRef]
15. Drake, G.W.F. Theoretical energies for the n = 1 and 2 states of the helium isoelectronic sequence up to Z = 100. *Can. J. Phys.* **1988**, *66*, 586. [CrossRef]
16. Yerokhin, V.A.; Pachucki, K. Theoretical energies of low-lying states of light helium-like ions. *Phys. Rev. A* **2010**, *81*, 022507. [CrossRef]
17. Yerokhin, V.A.; Shabaev, V.M. Lamb Shift of n = 1 and n = 2 States of Hydrogen-like Atoms, $1 \leq Z \leq 110$. *J. Phys. Ref. Data* **2015**, *44*, 3. [CrossRef]
18. Yerokhin, V.A.; Surzhykov, A. Theoretical Energy Levels of 1sns and 1snp States of Helium-Like Ions. *J. Phys. Chem. Ref. Data* **2019**, *48*, 033104. [CrossRef]
19. Yerokhin, V.A.; Patkóš, V.; Pachucki, K. QED calculations of energy levels of heliumlike ions with $5 \leq Z \leq 30$. *Phys. Rev. A* **2022**, *106*, 022815. [CrossRef]
20. Engström, L.; Litzén, U. High-precision wavelength measurements of the $1s^2\ ^1S$-$1snp\ ^1P$ resonance lines in He-like nitrogen and oxygen. *J. Phys. B* **1995**, *28*, 2565. [CrossRef]
21. Beiersdorfer, P. Precision energy-level measurements and QED of highly charged ions. *Can. J. Phys.* **2009**, *87*, 9. [CrossRef]
22. Reed, K.J.; Chen, M.H. Relativistic effects on the polarization of line radiation emitted from He-like and H-like ions following electron-impact excitation. *Phys. Rev. A* **1993**, *48*, 3644. [CrossRef] [PubMed]
23. Gu, M.F. The Flexible Atomic Code. In Proceedings of the Atomic Processes in Plasmas: 14th APS Topical Conference on Atomic Processes in Plasmas, Santa Fe, New Mexico, 19–22 April 2004; Volume 730, pp. 127–136.
24. Gu, M.F. The flexible atomic code. *Can. J. Phys.* **2008**, *86*, 675. [CrossRef]


**Disclaimer/Publisher's Note:** The statements, opinions and data contained in all publications are solely those of the individual author(s) and contributor(s) and not of MDPI and/or the editor(s). MDPI and/or the editor(s) disclaim responsibility for any injury to people or property resulting from any ideas, methods, instructions or products referred to in the content.